Available online at www.sciencedirect.com
ScienceDirect
Thermochimica Acta 465 (2007) 48–58
thermochimica acta
www.elsevier.com/locate/tca

Morphology, melting behavior, and non-isothermal crystallization of poly(butylene terephthalate)/poly(ethylene-*co*-methacrylic acid) blends

Jiann-Wen Huang [a,*], Ya-Lan Wen [b,c], Chiun-Chia Kang [d], Mou-Yung Yeh [e,f], Shaw-Bing Wen [b,c]

[a] *Department of Styling & Cosmetology, Tainan University of Technology, 529 Chung Cheng Rd., Yung Kang City 710, Taiwan, ROC*
[b] *Department of Nursing, Meiho Institute of Technology, 23 Ping Kuang Rd., Neipu Hsiang, Pingtung 912, Taiwan, ROC*
[c] *Department of Resources Engineering, National Cheng Kung University, No. 1, University Rd., Tainan City 701, Taiwan, ROC*
[d] *R&D Center, Hi-End Polymer Film Co., Ltd. 15-1 Sin Jhong Rd., Sin Ying City 730, Taiwan*
[e] *Department of Chemistry, National Cheng Kung University, No. 1, University Rd., Tainan City 701, Taiwan, ROC*
[f] *Sustainable Environment Research Centre, National Cheng Kung University, Taiwan, ROC*

Received 21 May 2007; received in revised form 16 September 2007; accepted 16 September 2007
Available online 21 September 2007

Abstract

The morphology, melting behavior, and non-isothermal crystallization of poly(butylene terephthalate) (PBT) and poly(ethylene-*co*-methacrylic acid) (PEMA) blends were studied with scanning electron microscopy, X-ray diffraction and differential scanning calorimetry (DSC). PEMA forms immiscible, yet compatible, blends with PBT. Subsequent DSC scans on melt-crystallized samples exhibited two melting endotherms (T_{mI} and T_{mII}). The presence of PEMA would facilitate the recrystallization during heating scan and retard PBT molecular chains to form a perfect crystal in cooling crystallization. The dispersion phases of molten PEMA acts as nucleating agents to enhance the crystallization rate of PBT. The solidified PBT could act as nucleating agents to enhance the crystallization of PEMA, but also retard the molecular mobility to reduce crystallization rate. The U^* and K_g of Hoffman–Lauritzen theory were also determined by Vyazovkin's methods to support the interpretation.

Keywords: Poly(butylene terephthalate); Poly(ethylene-*co*-methacrylic acid); Blend; Non-isothermal crystallization

1. Introduction

Poly(butylene terephthalate) (PBT) is an importance thermoplastic material for a large number of applications because of its good combination of properties, such as rigidity and solvent resistance. Polymer blending provides an easy approach to improve the properties of polymers rather than design and synthesize new polymers. Some polymers were blended in PBT to attain the desired properties, such as poly(ethylene octene) (PEO) [1–3], poly(acrylonitrile-*co*-butadiene-*co*-styrene)(ABS) [4–7], functionalized ethylene-propylene random copolymer [8,9], and poly (ethylene-*co*- glycidyl methacrylate) [10].

The physical properties of polymer blends strongly depend on their crystallization behavior and morphology. In a two-component polymer blend, if the crystallization temperature of one component is higher than that of the other component, then the former crystallizes in the presence of the molten state of the other component whereas the second component crystallizes in the presence of the solidified phase of the first component [11]. The presence of a second component either in the molten or solid state affects both the nucleation and crystal growth of the crystallizing polymer. Therefore, studying the morphology and crystallization of both components is desirable. Many articles have noted the effects of a second component on the crystallization of PBT in PBT blends [1–10]. However, the knowledge related to the effects on crystallization of a minor component is still scarce. Research on isothermal crystallization is limited to idealized conditions such as constant temperature; therefore, the theoretical analysis is relatively easy. Non-isothermal crystallization is a more complex process since temperature is not constant.

Semicrystalline poly(ethylene-*co*-methacrylic acid) copolymer (PEMA) is an ethylene and methacrylic acid copolymer resin. Due to the presence of the *co*-monomers, PEMA provides excellent adhesion to variety of both polar and non-polar sub-

* Corresponding author. Fax: +886 6 2433812.
E-mail address: jw.huang@msa.hinet.net (J.-W. Huang).

0040-6031/$ – see front matter © 2007 Elsevier B.V. All rights reserved.
doi:10.1016/j.tca.2007.09.004

strates [12]. In this article, PBT and PEMA were compounded in a twin-screw extruder. The crystalline structure and morphology were characterized by WAXS and scanning electron microscopy (SEM). The melting behaviors and non-isothermal crystallization of these specimens were measured by differential scanning calorimetry (DSC). The non-isothermal crystallization processes of PBT and PEMA in blends were delineated by modified Avrami, Ozawa, and Liu models. The activation energy and parameters of Hoffman–Lauritzen theory under a non-isothermal condition were also estimated by Vyazovkin's methods.

2. Experimental

2.1. Materials

Commercial grade poly(butylene terephthalate) (PBT) was supplied by Sam Yang Co., Ltd. (Seoul, Korea) under trade name Tribit® PBT-1500 with a melt flow index (MFI) of 215 g/10 min (250 °C × 5 kgf, ASTM D1238). Poly (ethylene-*co*- methacrylic acid) copolymer (PEMA) containing 12% methacrylic acid with a melt flow index (MFI) of 13.5 g/10 min (190 °C × 2.16 kgf, ASTM D1238), trade name: Nucrel® 1207, was produced by Du Pont (USA). All materials were used as received without purification.

2.2. Sample preparation

All materials were dried at 323 K in a vacuum oven for 6 h before compounding. PBT and 10, 30, and 50 wt.% PEMA were compounded with a twin-screw extruder (L/D = 32, D = 40 mm, Continent Machinery Company, Tainan, Taiwan; Model CM-MTE 32) at 553 K and 300 rpm to make polymer blends of PBT9/PEMA1, PBT7/PEMA3, and PBT5/PEMA5 blends, respectively. The rod extrudate was cooled in a water bath. As a base of comparison, the neat PBT and PEMA were also passed through the extruder at the same conditions.

2.3. Morphology

In order to characterize the morphology of the blends, the samples were fractured in liquid nitrogen and examined with scanning electron microscope (HITACHI, S-3500).

2.4. Wide-angle X-ray diffraction

Wide-angle X-ray diffraction (WAXD) were carried out using a Philips XRG-3000 generator with Ni filtered Cu Kα radiation (λ = 1.54 Å) which operated at an applied voltage of 30 kV and a current of 30 mA. The patterns were recorded at a scanning rate of 1°/min. over an angular range 10°–40°. The samples crystallized from the molten state (533 K) to room temperature at a cooling rate of 10 K/min.

2.5. Thermal measurements

The melting and crystallization behaviors of polymer blends were investigated with a differential scanning calorimetry, Perkin–Elmer Pyris-1 DSC calibrated using indium with samples weights of 8–10 mg. All operations were carried out in a nitrogen atmosphere. The samples were heated to 533 K and held in the molten state for 5 min to eliminate the influence of thermal history.

3. Results and discussion

3.1. Morphology

Morphology of a blend depends on whether the minor component has a lower or higher viscosity when the components have different melt viscosities. If the minor component has a lower viscosity than the major one, the minor component will be finely dispersed [13,14]. The cryogenically fractured surfaces of blends of PBT with PEMA are shown in Fig. 1a–c, in which, the size of the dispersed phase clearly increased when the content of PEMA increased from 10 to 50 wt.%. The particle size was rather uniform in PBT9/PEMA1 and PBT7/PEMA3; however, in the PBT5/PEMA5, size variation clearly increased. The sizes of dispersed phase of PBT9/PEMA1 and PBT7/PEMA3 were ca. 0.7 and 1 μm, respectively, and were not change significantly with the content of PEMA. The small and homogeneous dispersed phases are due to the interaction between hydroxyl groups of PBT and acid groups of PEMA, which induce partial miscibility. When the PEMA content increased to 50 wt.% (PBT5/PEMA5) as shown in Fig. 1c, the mean size of dispersed phase increased to ca. 5–7 μm as is usual in rubber-toughened blends [15,16], and exhibits a very sharp interface between PEMA domains and PBT matrix. PEMA domains have a spherical shape and there are numbers of voids from which the dispersed PEMA were pulled out. The result indicates that the interfacial interaction between PBT and PEMA is poorer at higher content of PEMA.

3.2. WAXD

The X-ray diffraction patterns of melt-crystallized samples are shown in Fig. 2 for PBT, PBT9/PEMA1, PBT7/PEMA3, PBT5/PEMA5, and PEMA. The characteristic X-ray peaks for pure PBT were observed at the scattering angles 2θ of ca. 16.0°, 17.2°, 20.6°, 23.3°, 25.2°, 29.3° and 31.1°, which correspond to the reflections from the (011), (010), (11̄1), (100), (111̄), (101), and (111̄) planes, respectively [17,18], as listed in Table 1. The PEMA shows a strong diffraction peak at 2θ = 21.5°. It could be observed (Fig. 2 and Table 1) that characteristic peaks of the blends were similar to those of pure PBT and no new characteristic peaks appear in X-ray patterns of the blends. The results suggest that the PBT and PEMA components in the blends crystallized independently, and there is no co-crystallization of both components. The dependency of crystallization can be clearly observed in the 50%/50% blend (PBT5/PEMA5), where a broad peak appeared in 20.6°–21.5°.

3.3. Melting behaviors

3.3.1. First scan

Fig. 3 shows the results of the first DSC scan of PBT/PEMA blends quenched in water after compounding in an extruder.

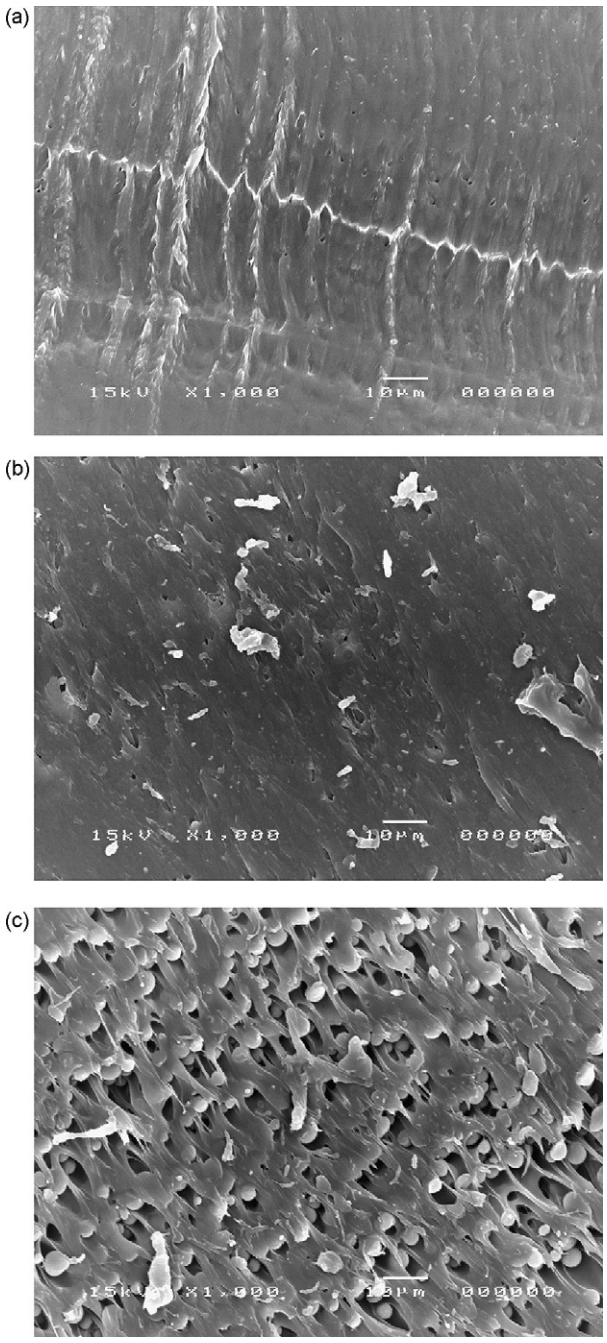

Fig. 1. SEM micrograph of PBT/PEMA blends. (a) PBT9/ PEMA1, (b) PBT7/PEMA3, (c) PBT5/PEMA5.

Two melting temperature of PBT (T_m^{PBT}) and PEMA (T_m^{PEMA}) are clearly observed, which implies they are immiscible. The T_m^{PBT} of all blends are 498.5, 498.5, 498.4, and 498.4 K for PBT, PBT9/PEMA1, PBT7/PEMA3, and PBT5/PEMA5, respectively. T_m^{PBT} does not change significantly with the addition of PEMA. The T_m^{PEMA} of neat PEMA is at 367.8 K, but that of PEMA in the PBT5/PEMA5, PBT7/PEMA3, and PBT9/PEMA1 appeared at 367.3, 366.8, and 365.8 K, respectively. T_m^{PEMA} decreases with the increasing content of PBT suggesting that the solidified PBT would retard the crystallization of PEMA [15].

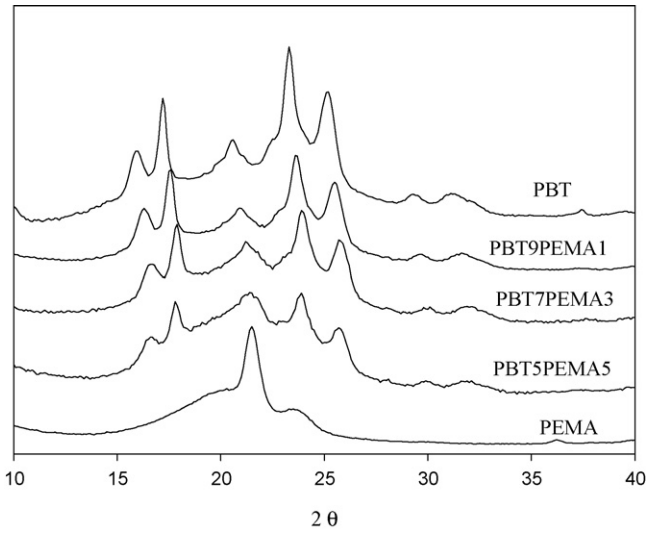

Fig. 2. WAXD patterns of PBT, PBT/PEMA blends, and PEMA.

3.3.2. *Influence of heating rate*

Fig. 4 shows the subsequent melting endotherms carried out at different heating rates (α) when samples were cooled at a cooling rate (Φ) of 10 K/min. from the molten state. The peak of T_m^{PEMA} (α = 10 K/min.) is similar to that of first scan; however, the peak of T_m^{PBT} spilt into two endothermic peaks (T_{mI}^{PBT} and T_{mII}^{PBT}). The two melting endotherms may be attributed to the melting of crystals with different structures [19,20] or that crystals have

Table 1
Peak positions (as equivalent Bragg spacings *d*) for PBT, PBT9/PEMA1, PBT7/PEMA3 and PBT5/PEMA5

Sample	Angle (2*θ*)	*d*-spacing (Å)	*hkl*
PBT	16.0	5.53	$(0\bar{1}1)$
	17.2	5.15	$(0\bar{1}0)$
	20.6	4.31	$(\bar{1}11)$
	23.3	3.81	$(1\bar{0}0)$
	25.2	3.53	$(\bar{1}11)$
	29.3	3.04	$(\bar{1}01)$
	31.1	2.87	$(\bar{1}\bar{1}1)$
PBT9/PEMA1	16.3	5.43	$(0\bar{1}1)$
	17.6	5.03	$(0\bar{1}0)$
	20.9	4.25	$(\bar{1}11)$
	23.6	3.77	$(1\bar{0}0)$
	25.5	3.49	$(\bar{1}11)$
	29.4	3.03	$(\bar{1}01)$
	31.6	2.83	$(\bar{1}\bar{1}1)$
PBT7/PEMA3	16.7	5.30	$(0\bar{1}1)$
	17.8	4.98	$(0\bar{1}0)$
	21.2	4.19	$(\bar{1}11)$
	23.9	3.72	$(1\bar{0}0)$
	25.7	3.46	$(\bar{1}11)$
	29.7	3.00	$(\bar{1}01)$
	31.8	2.81	$(\bar{1}\bar{1}1)$
PBT5/PEMA5	16.7	5.30	$(0\bar{1}1)$
	17.9	4.95	$(0\bar{1}0)$
	21.4	4.15	$(\bar{1}11)$
	23.9	3.72	$(1\bar{0}0)$
	25.8	3.45	$(\bar{1}11)$
	29.7	3.00	$(\bar{1}01)$
	31.9	2.80	$(\bar{1}\bar{1}1)$

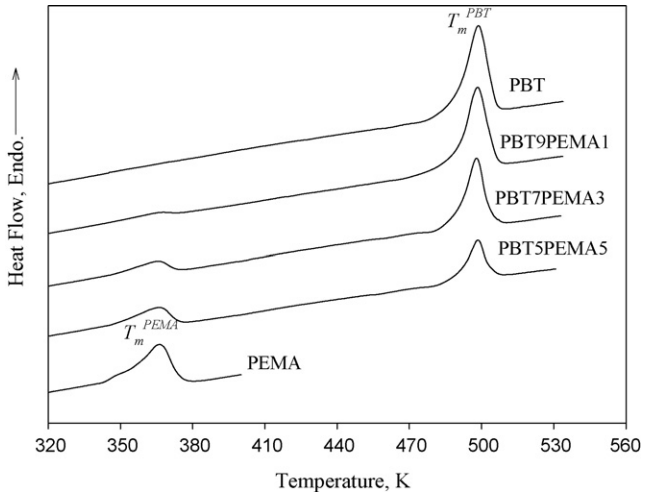

Fig. 3. First DSC heating scan of PBT, PBT/PEMA blends, and PEMA which were quenched in water after blending in an extruder. (Heating rate 10 K/min.)

a low degree of perfection, and that these crystals can partially melt and recrystallize during DSC scans to yield more perfect crystals [21,22]. The wide angle X-ray diffraction (Fig. 2) of all samples exhibit similar patterns and suggests that there are no additional phases associated with the two melting peaks. T_{mI}^{PBT} should be the peak associated with the fusion of the crystals grown by normal primary crystallization and T_{mII}^{PBT} is the melting peak of the more perfect crystals after reorganization during the heating process in DSC measurement.

It could be seen in Fig. 4, the peak intensity ratio of $T_{mI}^{PBT}/T_{mII}^{PBT}$ increased with the heating rate. During a melting and recrystallization process, if the less perfect crystallites passes through the recrystallization region rapidly, there is no sufficient time for the molten materials to reorganize into new crystals [23,24]. The higher the heating rate used, the shorter time being available for the diffusion of the molecular segments onto the growing crystallites [25]. The ratio of imperfect to perfect crystallites would increase at a higher heating rate. For a particular α, the peak intensity ratio of $T_{mI}^{PBT}/T_{mII}^{PBT}$ decreases with the increasing content of PEMA, it indicates that the dispersed phases of PEMA facilitate the recrystallization during heating scan.

3.3.3. Influence of cooling rate

Fig. 5 shows the DSC heating scans of neat PBT and PBT/PEMA blends at a heating rate of 10 K/min. after samples crystallized from molten state to room temperature with different cooling rate (Φ). The peaks of T_m^{PEMA} of PEMA in neat PEMA or PBT/PEMA blends do not change significantly when samples crystallized non-isothermally at different cooling rate. However, when the cooling rate decreases, T_{mI}^{PBT} moves to a higher temperature and the ratio of $T_{mI}^{PBT}/T_{mII}^{PBT}$ increase. It indicates that crystals with higher perfection grow in normal primary crystallization with a slower cooling rate. When the samples were crystallized at higher cooling rate, crystals with lower perfection formed and therefore are relatively prone to be organized during heating to a crystal population with a higher

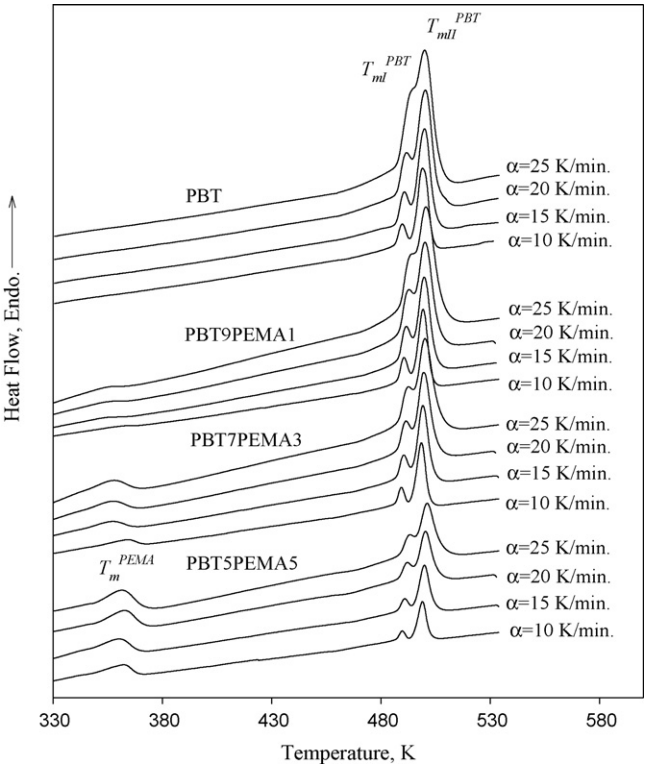

Fig. 4. Subsequent melting curves of PBT, PBT/PEMA at different heating rates after crystallization from the molten state at a cooling rate of 10 K/min.

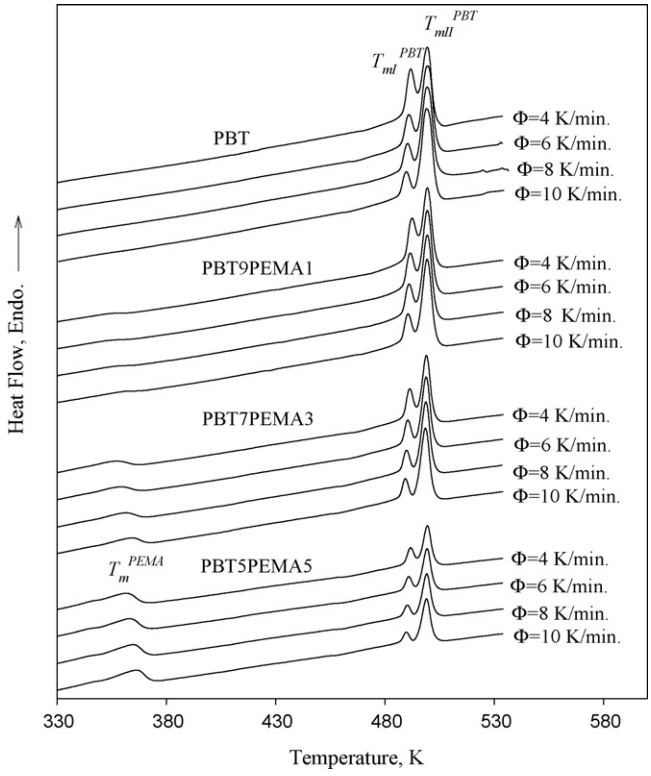

Fig. 5. Subsequent melting curves of PBT, PBT/PEMA blends, and PEMA at a heating rates of 10 K/min. after been non-isothermally crystallized from the molten state at various cooling rate (Φ).

thermodynamic stability. However, at slower cooling rate, the pre-existing crystals are much more perfect and less susceptible to reorganization [26].

At a specific cooling rate, the peak intensity ratio of $T_{mI}^{PBT}/T_{mII}^{PBT}$ decreases as content of PEMA increases; it indicates the PEMA retards PBT molecular chains to form a perfect crystals in primary crystallization and more imperfect crystals are susceptible to reorganization. The dispersed phases of PEMA act as nucleating agents to cause a large number of crystals to grow in a limited space. Therefore, the large number of nuclei causes more crystalline defects and more imperfect crystals were formed at a higher concentration of PEMA [27].

3.4. Non-isothermal crystallization

Fig. 6a–d shows DSC cooling traces at different cooling rate, and the values of DSC results are given in Table 2. All the DSC traces of the blends show two crystallization peaks, which indicate that these blends have two crystallizable components. PBT has a higher crystallization temperature than PEMA. The onset temperature of crystallization (T_o) and peak crystallization temperature (T_p) of PBT (T_o^{PBT} and T_p^{PBT}) shift to a higher temperature. The shifting indicates the immiscible dispersed phase of PEMA acts as heterogeneous nuclei and PBT starts to crystallize at a higher temperature. Similar behavior is observed in T_o of PEMA (T_o^{PEMA}), and PEMA starts to crystallize at a higher temperature as the content of PBT increases. The peak crystallization temperature of PEMA (T_p^{PEMA}) increases in the presence of 50 and 70 wt.% PBT (PBT5/PEMA5 and PBT7/PEMA3), then drops as additional PBT is added (PBT9/PEMA1). The solidified PBT acts as heterogeneous nuclei to enhance the crystallization of PEMA and therefore a higher T_o^{PEMA} is observed; but at the same time it also retards the crystallization at a higher content of PBT and a lower T_p^{PEMA} is observed in PBT9/PEMA1.

From DSC dynamic crystallization experiments, the data for the crystallization extherms as a function of temperature were obtained. Relative crystallinity (X_T) as a function of temperature was calculated as the ratio of the exothermic peak areas [28–30]:

$$X_T = \frac{\int_{T_o}^{T} [dH_c/dT]\,dT}{\int_{T_o}^{T_e} [dH_c/dT]\,dT} \quad (1)$$

where T is an arbitrary temperature, T_o is the onset temperature of crystallization, T_e is the temperature of crystallization com-

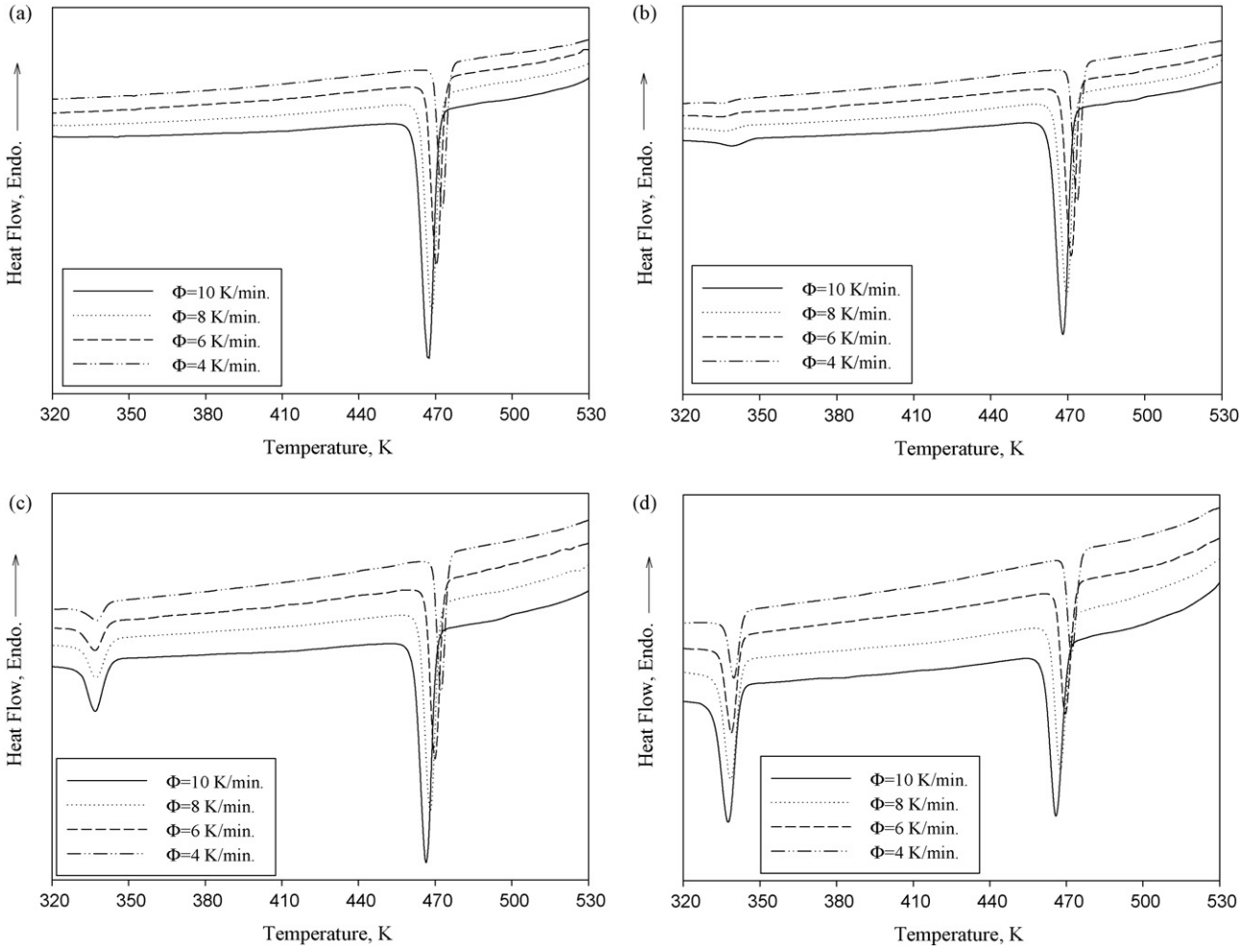

Fig. 6. DSC non-isothermal measurement curves for (a) PBT, (b) PBT9/PEMA1, (c) PBT7/PEMA3, (d) PBT5/ PEMA5.

Table 2
Characteristic data of non-isothermal melt crystallization exotherms for PBT and PBT/PEMA Blends

Sample	Φ (K/min)	T_o (K)		T_p (K)		$1/t_{1/2}$ (min^{-1})	
		T_o^{PBT}	T_o^{PEMA}	T_p^{PBT}	T_p^{PEMA}	PBT	PEMA
PBT	4	478.2	–	472.6	–	0.707	–
	6	477.1	–	470.3	–	0.862	–
	8	475.8	–	468.5	–	1.058	–
	10	474.9	–	467.3	–	1.216	–
PBT9/PEMA1	4	479.1	350.1	473.7	339.3	0.711	0.389
	6	477.4	349.3	471.3	339.2	0.948	0.570
	8	476.2	347.9	469.7	338.9	1.139	0.842
	10	475.8	347.2	468.2	337.0	1.223	0.927
PBT7/PEMA3	4	480.0	348.3	474.3	341.5	0.738	0.520
	6	477.8	347.7	471.9	339.8	1.004	0.726
	8	477.2	347.6	470.1	338.2	1.188	0.847
	10	476.3	345.3	468.6	338.3	1.342	1.049
PBT5/PEMA5	4	480.3	348.1	475.0	341.2	0.779	0.573
	6	478.8	347.6	472.6	340.2	1.106	0.772
	8	477.8	347.1	470.7	339.6	1.226	1.023
	10	477.1	345.0	468.9	338.6	1.487	1.437
PEMA	4	–	347.9	–	340.9	–	0.567
	6	–	347.4	–	339.6	–	0.746
	8	–	347.0	–	339.1	–	0.972
	10	–	345.9	–	337.8	–	1.165

pleted, dH_c is the enthalpy of crystallization released during an infinitesimal temperature interval dT. During the non-isothermal crystallization process, the time (t) and temperature exhibit the following relationship:

$$t = \left| \frac{T_o - T}{\Phi} \right| \tag{2}$$

where Φ is cooling rate. The temperature in Eq. (1) could be transformed into a timescale, X_t. Fig. 7 shows a typical relative crystallinity of PBT (X_t^{PBT}) in PBT5/EMA5 as a function of time. At higher cooling rate, less time is available to complete the crystallization.

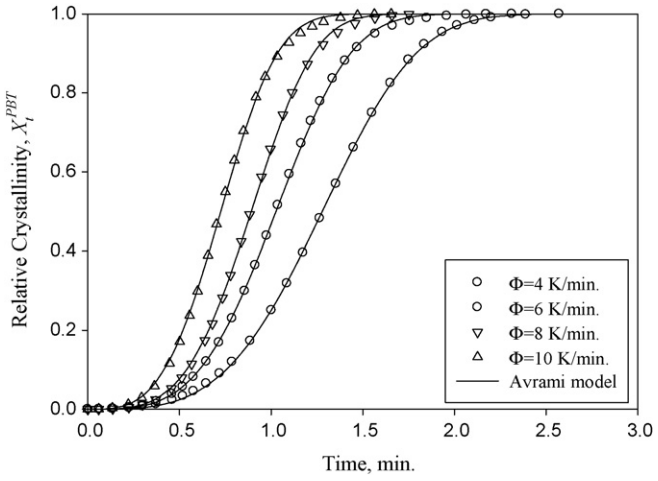

Fig. 7. Relative crystallinity, X_t^{PBT}, of PBT5/PEMA5 as a function of crystallization time at different cooling rate from experimental data and Avrami model.

Half-time ($t_{1/2}$) of the non-isothermal crystallization can be obtained with the following relationship:

$$t_{1/2} = \frac{|T_o - T_{1/2}|}{\Phi} \tag{3}$$

where $T_{1/2}$ is the temperature at which $X_T = 50\%$ and Φ is the cooling rate. The inverse value of $t_{1/2}$ (i.e., $1/t_{1/2}$) signifies the bulk crystallization rate and a lower $1/t_{1/2}$ value indicates slower crystallization. Table 2 also shows the $1/t_{1/2}$ for PBT and PEMA in blends. The $1/t_{1/2}$ value increases with increasing cooling rate indicating the polymer crystallized faster when the cooling rate was increased. For a particular Φ, the value of $1/t_{1/2}$ of PBT increases with the increasing content of PEMA. The immiscible dispersed phase of molten PEMA acts as nucleating agents to enhance the crystallization of PBT. The value of $1/t_{1/2}$ of PEMA also increases with the content of PBT, but drops at higher content (PBT9/PEMA1). It is due to the solidified PBT could act as nucleating agents to enhance the crystallization of PEMA, and retard the molecular mobility to reduce crystallization.

3.5. Avrami model

Many kinetic models have been proposed to study the non-isothermal crystallization of polymers. The most common approach is Avrami model [31–33] although there are some limitations [23]. The Avrami equation is expressed as:

$$X_t = 1 - \exp(-(K_a t)^{n_a}) \tag{4}$$

where X_t is the relative crystallinity, t is crystallization time, K_a is the Avrami crystallization rate constant and n_a is the Avrami exponent. X_t can be calculated as the ratio between the area of

Table 3a
Avrami kinetics parameters of PBT and PBT in PBT/PEMA blends

Sample	Cooling rate (K/min)	n_a^{PBT}	K_a^{PBT} (min^{-1})	K_J^{PBT}	R^2
PBT	4	3.98	0.641	0.895	0.9998
	6	4.17	0.781	0.960	0.9995
	8	3.95	0.949	0.998	0.9986
	10	3.81	1.081	1.008	0.9986
PBT9/PEMA1	4	4.25	0.645	0.896	0.9995
	6	3.90	0.851	0.973	0.9991
	8	3.83	1.021	1.003	0.9986
	10	3.93	1.091	1.009	0.9983
PBT7/PEMA3	4	4.25	0.647	0.897	0.9998
	6	3.92	0.974	0.996	0.9988
	8	3.97	1.051	1.006	0.9996
	10	4.02	1.117	1.011	0.9989
PBT5/PEMA5	4	3.57	0.706	0.917	0.9999
	6	3.99	0.993	0.999	0.9999
	8	3.83	1.136	1.016	0.9998
	10	3.89	1.237	1.021	0.9996

the exothermic peak at time t and the total measured area of crystallization. Values of K_a and n_a of PBT (K_a^{PBT} and n_a^{PBT}) and PEMA (K_a^{PEMA} and n_a^{PEMA}) were found by fitting experimental data of X_t^{PBT} and X_t^{PEMA} to Eq. (4) and the results were shown in Tables 3a and 3b. Avrami exponent (n_a) represents a parameter revealing the nucleation mechanism and growth dimension. The n_a^{PBT} values for neat PBT and PBT blends in Table 3a are 3.57–4.25, which indicates the addition of PEMA do not change the crystallization mechanism of PBT and means the crystallization mechanism is spherulite growth from sporadic (homogeneous) nucleation. The n_a^{PBT} value is similar to that reported by Wu [11], who found the n_a^{PBT} values 3.58–4.10. The n_a^{PEMA} values are 3.51–3.90 for neat PBT, PBT5/PEMA5, and PBT7/PEMA3, and reduced to 2.5–2.67 for PBT9/PEMA1. It implies that the crystallization changes from thermal nucleation and three-dimensional spherical growth to truncated spheres resulting from instantaneous nucleation with diffusion control.

Table 3b
Avrami kinetics parameters of PEMA and PEMA in PBT/PEMA blends

Sample	Cooling rate (K/min)	n_a^{PEMA}	K_a^{PEMA} (min^{-1})	K_J^{PEMA}	R^2
PEMA	4	3.90	0.5135	0.8465	0.9989
	6	3.79	0.6690	0.9352	0.9982
	8	3.66	0.8672	0.9823	0.9986
	10	3.54	1.034	1.0033	0.9985
PBT5/PEMA5	4	3.83	0.5455	0.8594	0.9977
	6	3.60	0.6823	0.9383	0.9988
	8	3.71	0.9081	0.9880	0..9980
	10	3.67	1.234	1.0212	0.9978
PBT7/PEMA3	4	3.68	0.4432	0.8159	0.9987
	6	3.57	0.6366	0.9275	0.9995
	8	3.68	0.7548	0.9654	0.9993
	10	3.51	1.152	1.0143	0.9973
PBT9/PEMA1	4	2.67	0.3478	0.7679	0.9995
	6	2.62	0.4887	0.8875	0.9995
	8	2.50	0.7223	0.9602	0.9998
	10	2.66	0.831	0.9817	0.9997

In non-isothermal crystallization K_a and n_a do not have the same physical significance as in the isothermal process because temperature deceased constantly in a non-isothermal process. This temperature changes may affect the rate of both nuclei formation and spherulite growth. However, Eq. (4) remains a good fit to experimental data based on regression coefficient (R^2) as can be seen in Tables 3a and 3b. The prediction according to the Avrami model is reconstructed in Fig. 7. From the comparison of the model prediction with experimental data, the Avrami model provides a good simulation below $X_t = 0.85$ for all samples, but exhibit an obvious deviation at higher X_t. It may be due to the neglect of secondary crystallization at higher X_t in Avrami model.

To meet the requirements of Avrami model, Jeziorny [34] assumed constant or approximately constant cooling rate and proposed the final form of the parameter characterizing the kinetics of a non-isothermal crystallization process:

$$\ln K_J = \frac{\ln K_a}{\Phi} \tag{5}$$

The values of K_J of PBT (K_J^{PBT}) and PEMA (K_J^{PEMA}) are listed in Tables 3a and 3b, and exhibit a similar trend as $1/t_{1/2}$.

3.6. Ozawa model

Considering the effect of cooling rate on the non-isothermal crystallization, Ozawa modified the Avrami model from isothermal crystallization to the non-isothermal crystallization by assuming that crystallization occurs at a constant cooling rate and the model as following [35]:

$$X_T = 1 - \exp\left[-\left(\frac{K_o}{\Phi}\right)^{n_o}\right] \tag{6a}$$

$$\ln\{-\ln[1 - X_T]\} = \ln K_o - n_o \ln \Phi \tag{6b}$$

Where K_o and n_o are Ozawa crystallization rate constant and Ozawa exponent, respectively. Fig. 8 illustrates a typical plot of $\ln[-\ln(1 - X_T)]$ as a function of $\ln \Phi$ for a fixed temperature. The K_o and n_o of PBT (K_o^{PBT} and n_o^{PBT}) and PEMA (K_o^{PEMA} and

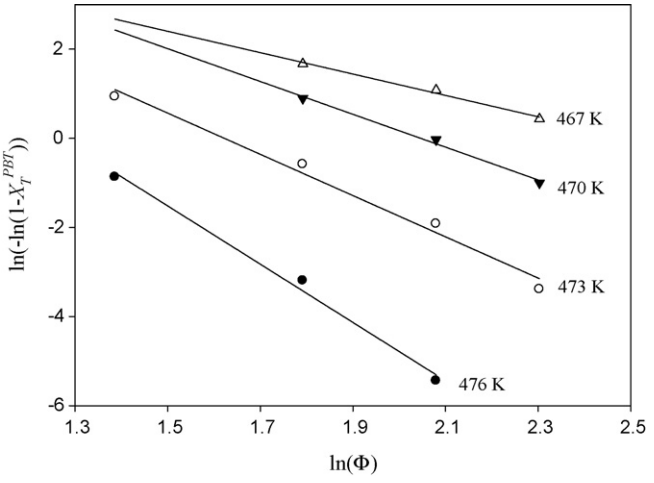

Fig. 8. Ozawa analysis based on the non-isothermal crystallization of PBT in PBT5/PEMA5.

Table 4a
Ozawa kinetic parameters of PBT and PBT in PBT/PEMA blends

Sample	Temperature (K)	n_a^{PBT}	K_o^{PBT}	R^2
PBT	473	5.91	3.63	0.9948
	470	4.03	4.96	0.9875
	467	2.43	8.57	0.9804
	464	1.97	13.92	0.9971
PBT9/PEMA1	473	6.04	4.12	0.9890
	470	3.63	6.10	0.9836
	467	2.58	9.76	0.9956
	464	1.77	16.22	0.9992
PBT7/PEMA3	476	7.77	3.24	0.9860
	473	5.63	4.36	0.9822
	470	3.49	6.85	0.9857
	467	2.46	10.99	0.9922
	464	1.99	16.96	0.9927
PBT5/PEMA5	476	6.54	3.56	0.9922
	473	4.63	5.07	0.9843
	470	3.68	7.76	0.9926
	467	2.40	12.20	0.9896

n_o^{PEMA}) could be estimated from the y-intercept (($K_o = \exp(y\text{-intercept}/n_o)$) and slope. The Ozawa kinetic parameters as well as regression coefficient (R^2) were listed in Tables 4a and 4b. Ozawa exponents were found to range from 1.77 to 7.77 for neat PBT and PBT in blends (n_o^{PBT}) within 464–476 K, and from 0.60 to 3.32 for PEMA and PEMA in blends (n_o^{PEMA}) within 332–344 K. The Ozawa exponent (n_o) is dependent on the dimension of crystal growth. Both n_o^{PBT} and n_o^{PEMA} increase with increasing crystallization temperature indicating the change of nucleation during the crystallization process [36]. But the n_o values listed in Tables 4a and 4b seem not reasonable, such as $n_o^{PBT} = 7.77$ and n_o^{PEMA}0.60 in PBT7/PEMA3. The scattering experimental data in Fig. 8, and the regression coefficient (R^2) listed in Tables 4a and 4b also show the Ozawa method is not suitable for describing the non-isothermal crystallization

Table 4b
Ozawa kinetic parameters of PEMA and PEMA in PBT/PEMA blends

Sample	Temperature (K)	n_o^{PEMA}	K_o^{PEMA}	R^2
PEMA	344	3.32	1.79	0.9226
	341	2.30	3.37	0.9509
	338	1.59	7.04	0.9638
	335	0.95	17.37	0.9509
	332	0.77	41.40	0.8954
PBT5/PEMA5	344	2.89	1.57	0.8499
	341	1.75	3.32	0.9642
	338	1.19	8.15	0.9620
	335	0.98	22.43	0.9407
	332	0.94	30.71	0.9121
PBT7/PEMA3	344	2.65	1.78	0.9588
	341	1.56	2.90	0.9837
	338	0.88	6.15	0.9507
	335	0.66	21.42	0.9095
	332	0.60	51.59	0.8118
PBT9/PEMA1	344	2.45	1.73	0.5846
	341	2.13	1.94	0.8144
	338	1.53	5.16	0.9260
	335	0.65	11.02	0.9206
	332	0.63	21.38	0.8544

of PBT/PEMA blend. Ozawa treatment is essentially quasi-isothermal in nature. The X_T chosen at a given temperature includes the values on the earliest stage as well as the values from the end stage of crystallization due to variation in the cooling rates. When the cooling rates vary in a wide range, the selected X_T values may have included secondary crystallization. The similar observations were also reported by Papageorgiou et al. [37].

3.7. Liu model

Liu et al. [38] combined Avrami and Ozawa models to deal with the non-isothermal crystallization behavior and its form is given as follow:

$$\ln \Phi = \ln \left[\frac{K_o^{n_o}}{K_a^{n_a}}\right]^{1/n_o} - \frac{n_a}{n_o} \ln t \tag{7a}$$

$$F(T) = \left[\frac{K_o^{n_o}}{K_a^{n_a}}\right]^{1/n_o} \tag{7b}$$

$$a = \frac{n_a}{n_o} \tag{7c}$$

Where the kinetic parameter, $F(T)$, refers to the value of the cooling rate chosen at the unit crystallization time when the measured system amounts to a certain degree of crystallinity; a is the ratio of Avrami exponent (n_a) to the Ozawa exponent (n_o). At a given degree of crystallinity, plotting $\ln \Phi$ versus $\ln t$ (Fig. 9) yielded a linear relationship between $\ln \Phi$ and $\ln t$ and the values of $F(T)$ and a of PBT(a^{PBT} and $F(T)_{PBT}$) and PEMA (a^{PEMA} and $F(T)_{PEMA}$) could be obtained from the slopes and intercepts of these lines, respectively. The value of a (in Table 5) varied from 1.53 to 2.12 for PBT in blends, 0.80 to 1.32 for PEMA in blends. The value of a for each sample almost keep constant. The value of $F(T)_{PBT}$ and $F(T)_{PEMA}$ increases with increasing degree of crystallinity indicating that at unit crystallization time, a higher cooling rate is required to reach a higher degree of crystallinity. At the same relative crystallinity, the order of $F(T)_{PBT}$ and $F(T)_{PEMA}$ are, respec-

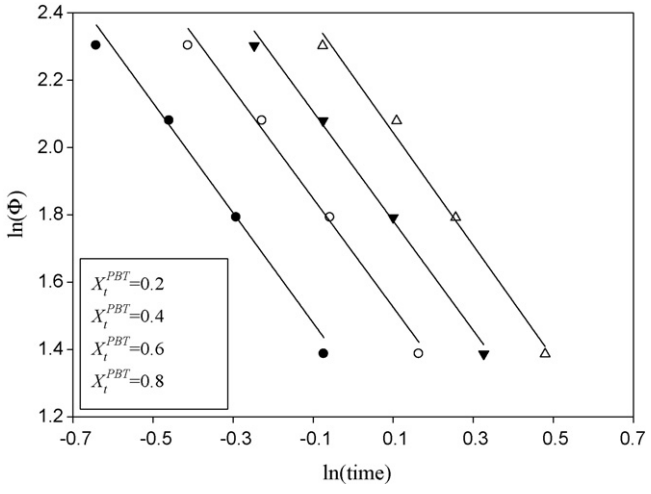

Fig. 9. Plots of $\ln \Phi$ verus $\ln t$ for different relative degree of crystallinity for PBT in PBT5/ PEMA5.

Table 5
Value of $F(T)$ and a for PBT, PEMA and PBT/PEMA Blends

Sample	X_t^{PBT}	$F(T)_{PBT}$	a_{PBT}	X_t^{PEMA}	$F(T)_{PEMA}$	a_{PEMA}
PBT	0.2	4.60	1.67	–	–	–
	0.4	6.48	1.65	–	–	–
	0.6	8.25	1.67	–	–	–
	0.8	10.88	1.74	–	–	–
PBT9/PEMA1	0.2	4.31	1.53	0.2	6.78	0.80
	0.4	5.71	1.54	0.4	8.67	0.84
	0.6	7.16	1.57	0.6	10.56	0.86
	0.8	9.31	1.63	0.8	12.97	0.87
PBT7/PEMA3	0.2	3.85	1.99	0.2	5.79	1.21
	0.4	5.62	2.01	0.4	8.00	1.24
	0.6	7.44	2.04	0.6	9.99	1.20
	0.8	10.34	2.12	0.8	13.50	1.28
PBT5/PEMA5	0.2	3.65	1.62	0.2	5.45	0.88
	0.4	5.35	1.60	0.4	6.88	0.87
	0.6	6.90	1.60	0.6	8.11	0.88
	0.8	9.12	1.67	0.8	9.68	0.88
PEMA	–	–	–	0.2	5.96	1.22
	–	–	–	0.4	7.57	1.24
	–	–	–	0.6	9.18	1.27
	–	–	–	0.8	11.54	1.32

tively, PBT > PBT9/PEMA1 > PBT7/PEMA3 > PBT5/PEMA5 and PBT9/PEMA1 > PEMA> PBT5/PEMA5 > PBT7/ PEMA3. The results further indicate that the crystallization of PBT in blends is ranked: PBT5/PEMA5 > PBT7/PEMA3 > PBT9 /PEMA1 > PBT, and PEMA in blends is ranked: PBT7/ PEMA3 > PBT5/PEMA5 > PEMA > PBT > PBT9/PEMA1. Similar rankings were obtained based on $1/t_{1/2}$ and K_J.

3.8. Effective activation energy

Several methods have been suggested to estimate the effective activation energy in non-isothermal crystallization [39–41]. However, to drop the negative sign in cooling process may result in errors [42]. The correct values can be determined by the differential isoconversional method of Friedman [43] and the advanced integral isoconversional method of Vyazovkin [44,45]. The Friedman equation [43] is applied to estimate the dependence of the effective activation energy on conversion in this study, and the Friedman equation could be expressed as follows:

$$\ln\left(\frac{dX_t}{dt}\right)_{X_t} = \text{constant} - \frac{\Delta E_{X_t}}{RT_{X_t}} \quad (8)$$

where $(dX_t/dt)_{X_t}$ is the instantaneous crystallization rate as a function of time for a given value of the relative crystallinity (X_t), R is the universal gas constant, and ΔE_{X_t} is the effective activation energy of the process for a given value of X_t. At various cooling rates, the values of dX_t/dt at a specific X_t are correlated to the corresponding crystallization temperature at this X_t, that is, T_{X_t} and a straight line can be obtained by plotting dX_t/dt versus $1/TXt$ with the slope $-\Delta E_{X_t}/R$.

The dependence of the effective activation energy of PBT ($\Delta E_{X_t}^{PBT}$) and PEMA ($\Delta E_{X_t}^{PEMA}$) in blends on conversion based on Friedman equation are shown in Fig. 10a and b. $\Delta E_{X_t}^{PBT}$ (or

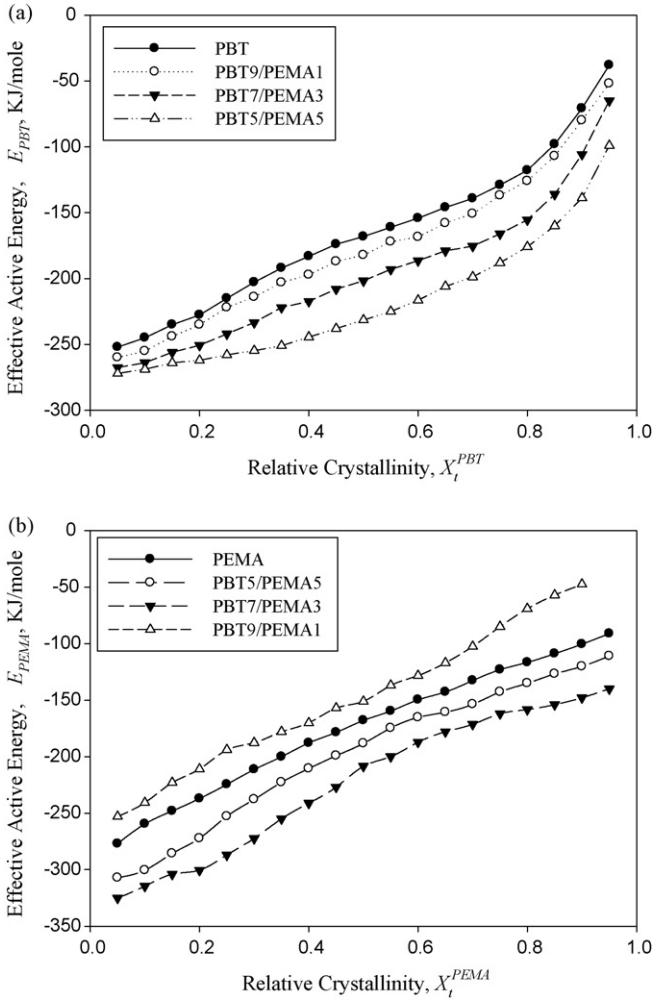

Fig. 10. Dependence of the effective energy barrier on the extent of relative crystallinity. (a) PBT and PBT in blends, $\Delta E_{X_t}^{PBT}$; (b) PEMA and PEMA in blends, $\Delta E_{X_t}^{PEMA}$.

$\Delta E_{X_t}^{PEMA}$) value for each resin is found to increase with increasing X_t^{PBT} (or X_t^{PEMA}) suggesting that, as the crystallization progressed, it is more difficult for the polymer to crystallize.

The dependence of the effective activation energy on temperature can be evaluated by replacing X_t with an average temperature, according to Vyazovkin's method [44,45], and the results are shown in Fig. 11a and b. The activation energy is negative, which indicates the crystallization increases with decreasing temperature.

Vyazovkin [44,45] used the results of the effective activation energy on temperature to estimate the parameters (K_g and U^*) of the Lauritzen–Hoffman theory [46] and derived the following equation:

$$\Delta E_{X_t} = -R\frac{(\ln G)}{d(1/T)} = U^*\frac{T^2}{(T-T_\infty)^2} + K_g R\frac{(T_m^o)^2 - T^2 - T_m^o T}{(T_m^o - T)^2 T} \quad (9)$$

K_g is the nucleation parameter, which can be related to the product of lateral (σ) and folding surface free energy (σ_e); U^* is

Table 6
Crystallization parameters of PBT

	$K_g^{PBT} \times 10^5$ (K^2)	U^{*PBT} (J/mole)	R^2	$K_g^{PBT} \times 10^5$ (K^2)	U^{*PEMA} (J/mole)	R^2
PBT	2.49	11364	0.9855	–	–	–
PBT9/PEMA1	2.39	11156	0.9903	5.09	11769	0.9965
PBT7/PEMA3	1.98	8774	0.9826	3.88	5762	0.9958
PBT5/PEMA5	1.85	8313	0.9815	4.47	8307	0.9968
PEMA	–	–	–	4.73	9852	0.9825

the diffusional activation energy for the transport of crystallizable segments at the liquid-solid interface; R is the gas constant; $T_\infty = T_g - 30$ K is the hypothetical temperature below which viscous flow ceases and T_g is glass transition temperature; T_m^o is the equilibrium melting temperature. T_g and T_m^o are 248 K [47] and 509 K [48] for PBT, 153 and 388 K [49] for PEMA. The values K_g and U^* can be estimated by fitting Eq. (9) with the results of dependence of the effective activation energy on temperature, and the results are shown in Table 6. The K_g^{PBT} value (2.49×10^5) of neat PBT estimated by Eq. (9) is similar to those reported by Di Lorenzo (2.72×10^5) [47] and Chen (2.02×10^5) [26], which were estimated from isothermal crystallization. Vyazovkin's equation seems to provide a good method to estimate the K_g value under non-isothermal crystallization.

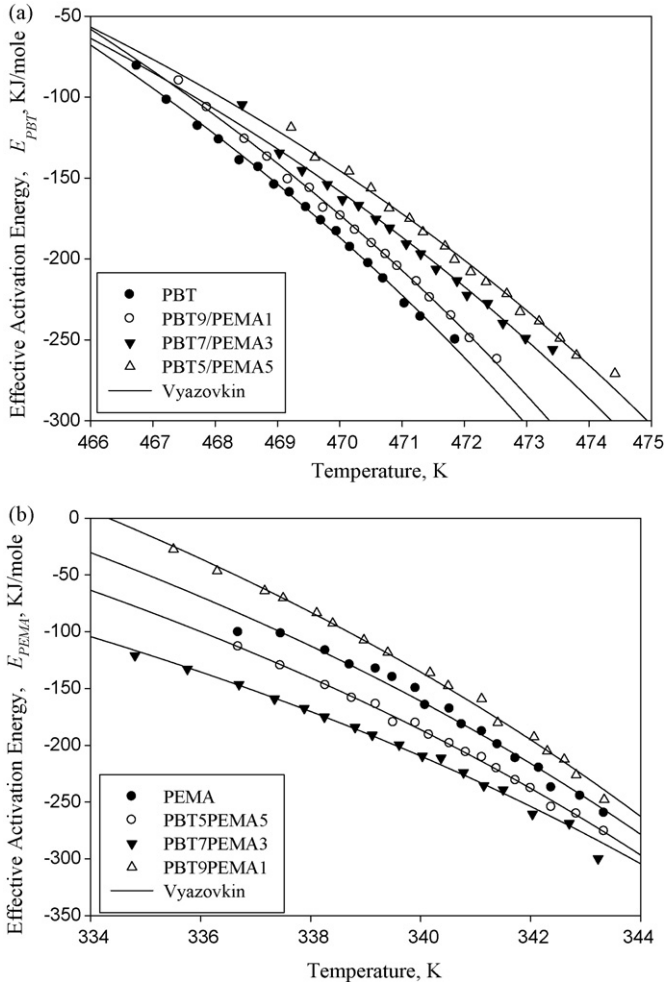

Fig. 11. Dependence of the effective activation energy on average temperature and fitted by Vyazovkin equation. (a) PBT and PBT in blends, $\Delta E_{X_t}^{PBT}$; (b) PEMA and PEMA in blends, $\Delta E_{X_t}^{PEMA}$.

Both $\Delta E_{X_t}^{PBT}$ and K_g^{PBT} values decrease with increasing content of PEMA, and it indicates the addition of more PEMA into the PBT matrix causes more heterogeneous nucleation to enhance crystallization. The values of $\Delta E_{X_t}^{PEMA}$ and K_g^{PEMA} in PBT5/PEMA5 and PBT7/PEMA3 is lower than those of neat PEMA. However, both values in PBT9/PEMA1 are higher than those of neat PEMA. It seems that the solidified PBT confines the molecular mobility of PEMA to reduce the crystallization rate in PBT9/PEMA1. The higher U^{*PEMA} of PBT9/PEMA1 than those of other blends also confirms the results. High U^* value suggests that the diffusion is more difficult in PBT9/PEMA1. Hoffman [46] has estimated the range of U^* to vary between 4200 and 16700 J/mol. The values of U^* in Table 6 are consistent with the range and seem reasonable.

4. Conclusion

The PBT and PEMA were compounded in a twin-screw extruder. PEMA forms immiscible, yet compatible, blends with PBT through interaction between carbonyl acid groups and hydroxyl groups of PBT at lower content of PEMA (<30 wt.%). The immiscible PEMA was dispersed homogeneously in PBT9/PEMA1 and PBT7/PEMA3, but heterogeneously in PBT5/PEMA5. The blending of PEMA to PBT does not affect the melting process of the PBT quenched from molten state. Subsequent DSC scans of non-isothermally crystallized samples exhibit two melting endotherms due to melt-recrystallization. The lower temperature (T_{mI}) is associated with the fusion of the crystals grown by normal primary crystallization and the higher one (T_{mII}) is the melting peak of the more perfect crystals reorganized during the DSC heating scan. At higher heating rate, the less perfect crystallites passes through the recrystallization region rapidly that there is no sufficient time for the molten materials to reorganize into new crystals, and the intensity of T_{mII} decreases. At lower cooling rate, the existing more perfect crystals are less susceptible to reorganization and the intensity of T_{mII} decreases. The non-isothermal crystallization processes of PBT and PEMA in blends were delineated by modified Avrami, Ozawa, and Liu models. Ozawa model seems not suitable to describe the crystallization process of PBT and PEMA. All the crystallization kinetics parameters ($1/t_{1/2}$, K_J, and $F(t)$) indicate the crystallization rate of PBT increases with increasing content of PEMA. The dispersion phases of molten PEMA acts as nucleating agents to enhance the crystallization rate of PBT. The

crystallization rate of PEMA increases with increasing content of PBT up to 30 wt.%, and then decreases at higher content of PBT. The solidified PBT acted as nucleating agents to enhance the crystallization of PEMA, but also retarded the molecular mobility to reduce crystallization at higher PBT content. Such interpretation was supported by the effective activation energy (ΔE_{X_t}) and the nucleation parameter (K_g) calculated by Vyazovkin's method.

References

[1] A. Aróstegui, M. Gaztelumendi, J. Nazábal, Polymer 42 (2001) 9565.
[2] G. Guerrica-Echevarria, J.I. Eguiazabal, J. Nazabal, Polym. Eng. Sci. 46 (2006) 172.
[3] A. Aróstegui, J. Nazábal, Polym. Eng. Sci. 43 (2003) 1691.
[4] W. Hale, H. Keskkula, D.R. Paul, Polymer 40 (1999) 365.
[5] W. Hale, H. Keskkula, D.R. Paul, Polymer 40 (1999) 3665.
[6] W.R. Hale, L.A. Pessan, H. Keskkula, D.R. Paul, Polymer 40 (1999) 4237.
[7] W. Hale, J.H. Lee, H. Keskkula, D.R. Paul, Polymer 40 (1999) 3621.
[8] A. Cecere, R. Greco, G. Ragosta, G. Scarinzi, A. Taglialatela, Polymer 31 (1990) 1239.
[9] P. Vongpanish, A.K. Bhowmick, T. Inoue, Plast. Rubber Comp. Proc. Appl. 21 (1994) 109.
[10] A. Aróstegui, J. Nazábal, J. Polym. Sci. Polym. Phys. 41 (2003) 2236.
[11] D. Wu, C. Zhou, X. Fan, D. Mao, Z. Bian, J. Appl. Polym. Sci. 99 (2006) 3257.
[12] N. Somrang, M. Nithitanakul, B.P. Grady, P. Supaphol, Euro. Polym. J. 40 (2004) 829.
[13] J. Runt, D.M. Miley, X. Zhang, K.P. Gallagher, K. McFeaters, J. Fisburn, Macromolecules 25 (1992) 1929.
[14] K. Palanivelu, P. Sivaraman, M.D. Reddy, Polym. Test. 21 (2002) 345.
[15] A. Aróstegui, J. Nazábal, Polymer 44 (2003) 239.
[16] H. Chen, B. Yang, H. Zhang, J. Appl. Polym. Sci. 77 (2000) 928.
[17] B. Wang, Y.C. Li, J. Hanzlicek, S.Z.D. Cheng, P.H. Geil, J. Grebowicz, R.M. Ho, Polymer 42 (2001) 7171.
[18] A.S. Liu, W.B. Liau, W.Y. Chiu, Macromolecules 77 (1998) 6593.
[19] R.C. Roberts, Polymer 10 (1969) 113.
[20] R.C. Roberts, Polymer 10 (1969) 117.
[21] J.T. Yeh, J. Runt, J. Polym. Sci. Polym. Phys. Ed. 27 (1989) 1543.
[22] M.E. Nichols, R.E. Robertson, J. Polym. Sci. Polym. Phys. Ed. 30 (1992) 305.
[23] B. Wunderlich, Macromolecular Physics, vol. 3, Academic, New York, 1980.
[24] Y. Wang, M. Bhattacharya, J. Mano, J. Polym. Sci. Polym. Phys. 43 (2005) 3077.
[25] P. Srimoaon, N. Dangseeyun, P. Supaphol, Euro. Polym. J. 40 (2004) 599.
[26] X. Chen, J. Xu, H. Lu, Y. Yang, J. Polym. Sci. Polym. Phys. 44 (2006) 2112.
[27] J. Gao, D. Wang, M. Yu, Z. Yao, J. Appl. Polym. Sci. 93 (2004) 1203.
[28] J.N. Hay, M. Sabir, Polymer 10 (1969) 203.
[29] J.N. Hay, P.A. Fitzgerald, M. Wiles, Polymer 17 (1976) 1015.
[30] J.N. Hay, Bri. Polym. J. 11 (1979) 137.
[31] M.J. Avrami, J. Chem. Phys. 7 (1939) 1103.
[32] M.J. Avrami, J. Chem. Phys. 8 (1940) 212.
[33] M.J. Avrami, J. Chem. Phys. 9 (1941) 177.
[34] A. Jeziorny, Polymer 19 (1978) 1142.
[35] T. Ozawa, Polymer 12 (1971) 150.
[36] Z. Qui, S. Fujinami, M. Komura, K. Nakajima, T. Ikehara, T. Nishi, Polym. J. 36 (2004) 642.
[37] G.Z. Papageorgiou, D.S. Achilias, D.N. Bikiaris, G.P. Karayannidis, Thermochim. Acta 427 (2005) 117.
[38] T.X. Liu, Z.S. Mo, S.E. Wang, H.F. Zhang, Polym. Eng. Sci. 37 (1997) 568.
[39] J.A. Augis, J.E. Bennett, J. Therm. Anal. 13 (1978) 283.
[40] H.E. Kissinger, J. Res. Natl. Bur. Stand. 57 (1956) 217.
[41] R.L. Takhor, Advances in Nucleation and Crystallization of Glasses, American Chemical Society, Columbus, 1971.
[42] S. Vyazovkin, N. Sbirrazzuoli, J. Phys. Chem. B 107 (2003) 882.
[43] H. Friedman, J. Polym. Sci. Polym. Symp. 6 (1964) 183.
[44] S. Vyazovkin, N. Sbirrazzuoli, Macromol. Rapid Commun. 25 (2004) 733.
[45] S. Vyazovkin, I. Dranca, Macromol. Chem. Phys. 207 (2006) 20.
[46] J.D. Hoffman, G.T. Davis, J.I. Lauritzen Jr., in: N.B. Hannay (Ed.), Treatise on Solid State Chemistry, vol. 3, Plenum, NY, 1976, p. 479.
[47] M.L. Di Lorenzo, M.C. Righetti, Polym. Eng. Sci. 43 (2003) 1889.
[48] J. Runt, D.M. Milley, X. Zhang, K.P. Gallagher, K. McFeaters, J. Fishburn, Macromolecules 25 (1992) 1929.
[49] J. W. Huang, unpublished results.